Molecular Dynamics Simulation of the Structural and Dynamic Properties of Dioctadecyldimethyl Ammoniums in Organoclays

Q. H. Zeng,[†] A. B. Yu,*[,†] G. Q. Lu,[#] and R. K. Standish[‡]

Centre for Simulation and Modeling of Particulate Systems, School of Materials Science and Engineering, The University of New South Wales, Sydney, NSW 2052, Australia, ARC Centre for Functional Nanomaterials, School of Engineering, The University of Queensland, Brisbane, QLD 4072, Australia, and School of Mathematics, The University of New South Wales, Sydney, NSW 2052, Australia

Received: October 27, 2003; In Final Form: March 23, 2004

The structural and dynamic properties of dioctadecyldimethylammoniums (DODDMA) intercalated into 2:1 layered clays are investigated using isothermal−isobaric (NPT) molecular dynamics (MD) simulation. The simulated results are in reasonably good agreement with the available experimental measurements, such as X-ray diffraction (XRD), atom force microscopy (AFM), Fourier transform infrared (FTIR), and nuclear magnetic resonance (NMR) spectroscopies. The nitrogen atoms are found to be located mainly within two layers close to the clay surface whereas methylene groups form a pseudoquadrilayer structure. The results of tilt angle and order parameter show that interior two-bond segments of alkyl chains prefer an arrangement parallel to the clay surface, whereas the segments toward end groups adopt a random orientation. In addition, the alkyl chains within the layer structure lie almost parallel to the clay surface whereas those out of the layer structure are essentially perpendicular to the surface. The trans conformations are predominant in all cases although extensive gauche conformations are observed, which is in agreement with previous simulations on *n*-butane. Moreover, an odd−even effect in conformation distributions is observed mainly along the chains close to the head and tail groups. The diffusion constants of both nitrogen atoms and methylene groups in these nanoconfined alkyl chains increase with the temperature and methelene position toward the tail groups.

Introduction

Intercalation of nonionic, cationic, and anionic surfactants in layered solids has been a subject of considerable interest.[1−3] The structural and dynamic properties of intercalated surfactants are known to be markedly different from those in bulk. The most prominent feature for surfactants at surfaces and confined between two solid surfaces is that the surfactants tend to organize into layered structures in the direction normal to the surface. Such structures are observed in the Langmuir−Blodgett films and intercalated surfactants in layered solids. For example, it is well-known that the fluid density of films with the thickness of a few molecular diameters is not uniform across the film, but instead shows an oscillatory profile. In addition, the confined thin films show a more solidlike behavior. Understanding the molecular origin of confinement-induced changes is of fundamental and technical importance in many processes such as lubrication, adhesion, coating, chromatography, membrane separation, and fabrication of polymer nanocomposites.[4−7] The organization and orientation of these confined surfactants have therefore been a subject of interest for many years. Extensive theoretical[7−26] and experimental[27−30] studies have been reported on confined molecules, particularly at a single-sided wall. However, to date very few experimental studies have been reported on surfactants intercalated into the galleries of layered solids due to the experimental difficulties,[31−37] some of which are discussed below.

So far, X-ray diffraction (XRD) is the most widely used technique to determine the layered structure and orientation of intercalated surfactants, which is based on the basal spacing and the assumption that all the surfactant chains have all-trans conformations. Although various structural models have been proposed for the intercalated surfactants, they do not directly reveal the significant structural characteristics of the surfactants, that is, the coexistence of trans and gauche conformations.[38] More recently, Fourier transform infrared (FTIR) spectroscopy has been used to probe the structure and phase state of intercalated surfactants in layered solids by monitoring the frequency shifts of methylene on alkyl chains.[32,37] The FTIR results show the substantial existence of gauche conformation even though the trans conformation is still predominant in most conditions. Nevertheless, FTIR provides little information on the dynamics of molecular chains. In view of this, nuclear magnetic resonance (NMR) spectroscopy has been proven to be one of the most powerful techniques for probing structure and conformation, as well as dynamics of surfactants at surfaces and confined between two solid surfaces. In fact, recent NMR studies on intercalated surfactants in layered solids further clarified the coexistence of ordered trans and disordered gauche conformations, and showed that the methylene units of surfactant chains in the galleries of layered solids are more mobile as compared to those in the crystalline state, which may be explained from the greater conformational freedom resulting from the relatively low packing density.[34,37] However, to date the structural, conformational, and dynamic information of these intercalated surfactants is still difficult to be experimentally quantified. For instance, it is difficult to deduce the orientation

* Corresponding author, telephone: 61 2 9385 4429, fax: 61 2 9385 5956, E-mail: a.yu@unsw.edu.au.

[†] School of Materials Science and Engineering, The University of New South Wales.

[#] School of Engineering, The University of Queensland.

[‡] School of Mathematics, The University of New South Wales.

10.1021/jp037245t CCC: $27.50
Published on Web 06/15/2004

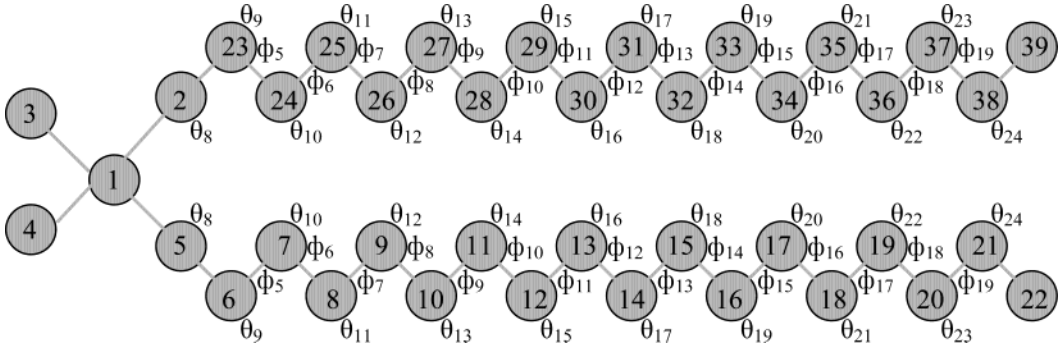

Figure 1. Schematic of the DODDMA chain. The group numbers are given within the circles. The groups include methyl (2, 5−21, 23−38), methylene (3, 4, 22, 39), and nitrogen. The bond angles (θ) and torsion angles (ϕ) used in the subsequent analysis are indicated, respectively. For instance, θ_9 corresponds to 5−6−7 and/or 2−23−24. Also, ϕ_5 corresponds to 5−6−7−8 and/or 2−23−24−25.

of the alkyl chains with respect to the solid surface from physical experiments.

Computer simulation provides a powerful alternative to probing the structural and dynamic properties at a molecular level, and offers a direct connection between microscopic details and macroscopic properties of a considered system. In particular, simulations of nanoconfined molecules have revealed many dramatically different properties from the bulk molecules, such as the structure, local relaxation,[39] mobility,[40] and rheological properties.[41] However, the molecular confinement may exist in various geometries or porous media, such as zeolites or graphite.[42,43] In the case of confinement in layered solids, as we are concerned with here, many computer simulations have been done for small molecules, which provides detailed information about the behavior of the molecules. In contrast, few studies have been done for long chain molecules and polymers. For example, Molecular Dynamic (MD) simulations have been extensively used in the past decade to investigate the behaviors of confined molecules. However, previous studies were mainly restricted to systems in which the molecules are confined between two structured or structureless surfaces.[8−25]

Intercalation compounds provide an ideal model system to study the behavior of surfactants within a nanoconfined environment. As far as we know, only a few MD simulation studies have been reported on surfactants intercalated into the galleries of layered solids.[25,26] Recently we used MD simulation to investigate the layering structure of quaternary alkylammoniums intercalated into clays.[44] A variety of structures are found in organoclays with quaternary ammoniums containing a single long alkyl chain, including monolayers, bilayers, and pseudotrilayers depending on the chain length and clay layer charge. A pseudoquadrilayer structure has been observed in organoclays with quaternary ammoniums containing two long alkyl chains. Furthermore, surfactant chains in multilayer structures do not lie flat within a single layer but interlace and even jump to the next, as well as the next nearest, layers. In this study, we extend that work by quantifying the structure of the intercalated quaternary DODDMA chains in montmorillonite in terms of atomic density profile, alkyl alignment, order parameter, chain configuration, and trans and gauche conformation ratio and dynamic properties.

Simulation Method

The simulation method is same as that used in our previous work.[44] As such, we only describe briefly the initial configuration, force field, and simulation conditions as follows. The atomic coordinates for montmorillonite are derived from a simulated structural model proposed by Viani et al.[45] whose unit cell parameters are $a = 5.18$ Å, $b = 8.95$ Å, $c = 15.0$ Å, and $\alpha = \beta = \gamma = 90°$. The hydroxyl groups and magnesium ions are added to this model framework. The cation exchange capacity (CEC), which is a characteristic of the clay and is relative to the layer charge, determines the number of compensating cations in the gallery. Clays with various layer charges ($x = 0.625$, 0.75, or 0.875) have been constructed which correspond to various CECs (85, 102, or 119 milliequevalent/100 g of the clay). Our MD simulation cell with three periodic boundary conditions consists of 64 unit cells ($8 \times 4 \times 2$), resulting in an overall size of 41.44 Å × 35.92 Å. The third dimension is chosen close to the experimental results.[46,47] The interlayer cations are fully replaced by DODDMA chains. The schematic of the DODDMA chain is shown in Figure 1. The alkyl chains are built using the united atoms in which carbon atoms are made to adsorb the hydrogens in methyl and methylene groups. In the case of a fully-extended conformation, the chain length, for example, from atom 5 to 22, is about 21.25 Å as estimated according to the force-field parameters used in the present work. These parameters are the bond length of C−C (1.53 Å) and bond angle of C−C−C (109.47°). This length does not include the contributions of C−N (1.46 Å) and C−H (1.09 Å) bonds on both sides of the chain, which should be 1.15 and 0.89 Å, respectively.

The force field is a modified Dreiding force field.[48] It consists of a sum of potential energy terms, such as bond stretching, bond-angle bend, dihedral angle torsion, van der Waals energy, and electrostatic energy. Since the Dreiding force field does not contain parameters for Mg atoms, Mg is assigned the same parameters as Al except for the formal charges and its equilibrium bond length with oxygen (2.100 Å). In addition, the parameters for quaternary nitrogen are equal to those of N_3 in the Dreiding force field. The charges of atoms in clay are the same as those reported by Skipper et al.[49] The atomic charges of DODDMA chains are assigned by a charge equilibration method.[44,50] The one unit positive charge is assigned to the head group containing one nitrogen and its adjacent carbon atoms.

All simulations are performed using the DL_POLY program[51] on a SGI supercomputer whereas most data analysis is carried out using in-house programs developed specifically for this nanoconfined system. The MD algorithm is in the form of the Verlet leapfrog integration algorithm. To relax the model structures, simulations are first performed in the canonical (NVT) ensembles for 200 ps (picoseconds) at 300 K with a time step of 0.001 ps. The NPT simulations are then performed for 800 ps at 300 K except for those indicated and 10^5 Pa (1 atm) with a time step of 0.001 ps. The first 400 ps run is chosen to ensure that the system reaches its equilibrium, and the last 400 ps run is used to generate data for structural and dynamic analysis. The electrostatic interaction is calculated by the Ewald

sum method.[52] Temperature and pressure are maintained respectively by using the Hoover thermostat and barostat with a relaxation time of 0.5 ps.[53] During each run of the simulation the atom positions of clay are fixed while the alkyl chains are allowed to move.

Results and Discussion

The simulation method described above has been verified in our previous study on organoclays.[44] In the organoclays, the sodium cations are completely exchanged by alkylammoniums. In the case of DODDMA clays, we observed that the simulated basal spacings are increased from 25.6 to 27.3 and 29.1 Å with the increase of CECs from 85 to 102 and 119 meq/100 g. The data agree well with the experimental measurements reported in the range of 25.2−30.0 Å for these organoclays with equivalent CECs.[43,47,54−55] This is particularly true considering the fact that the measured basal spacings reported in the literature are rather scattered.

In this paper, we investigate the structure and dynamics of DODDMA chains intercalated into the interlayer spaces of two clay layers in a number of ways, including atom density profiles with respect to the z position, tilt angle, order parameter, and conformation and dynamic properties, averaged over 400 ps. Whenever possible, comparisons between simulated and measured results will be made, providing further evidence to confirm the validity of the proposed MD approach.

Layering Behavior and Density Profiles. To establish the structure of intercalated quaternary alkyl chains in clays, we began our analysis with the density profiles of nitrogen and methylene groups for three systems with CEC 85, 102 and 119 meq/100 g clay, recorded as a function of the distance from the gallery center in the direction normal to the clay surface. Such information is not available from the previous experimental work and structural models. Recently, Hacket et al.[25] reported their simulation work on organoclays modified with primary alkylammoniums. They pointed out that nitrogen groups were bound more closely to flat walls than methylene groups though there were no density distribution data for nitrogen groups. In the present study on quaternary alkylammoniums, the nitrogen groups as shown in Figure 2a are distributed throughout the whole interlayer space. However, they are mainly located within two layers in the proximity of the clay surface, exhibited by the two sharp peaks whose positions relative to the surface are conserved even with the increase of the layer charge of clays. These density profiles can be attributed to the strong electrostatic interactions between the negative clay surfaces and positive head groups of the alkyl chains, including the nitrogen and its adjacent methyls and methylenes.

The interlayer structure of organoclays is indicated largely on the arrangement of methylene groups in the long alkyl chains. Layering behavior has been found in the gallery of organoclays that is to some extent different from those of confined alkanes. In a simulation study on hexadane film, Gao et al.[24] reported four well-formed layers in the systems in which the hexadane film is confined between two solid surfaces separated by 18−22 Å. In the organoclays, the methylene density profiles in Figure 2b also show a similar layering behavior. The alkyl chains appear to be well layered throughout with four well-formed layers parallel to the clay surface. However, further analysis indicates that these profiles of intercalated DODDMA chains actually demonstrate an overall pseudoquadrilayer structure in which the methylene groups are likely to jump to the second layer and even extend to the third layer. As we can seen in Figure 2b, the density minima between the layers are larger

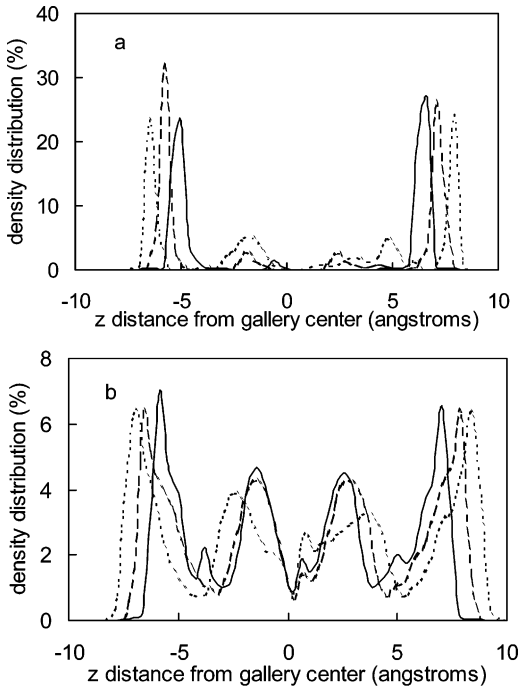

Figure 2. Density profiles of DODDMA-clays as a function of *z* distance from the gallery center: (a) nitrogen, (b) methylene. Solid curve, CEC 85 meq/100 g; dashed curve, CEC 102 meq/100 g; dotted curve, CEC 119 meq/100 g.

than zero, not close to zero as indicated in the simulation study of confined hexadane chains. Thus it is possible for one end (usually the head group) of the alkyl chain to be in the first layer (closest to the clay surface) and the other end to be located in the first, second, or third layer. From this point of view, the layering behavior in our case is quite different from that reported for confined hexadane.[24] To view this structure behavior, we will display in our later discussion only half of the DODDMA chains that radiate from the same side of the clay layers. In addition to the layered structure, the density of alkyl chains is found to oscillate with the distance normal to the surface, occurring with a periodicity of about 4−5 Å. Such an oscillatory behavior can explain the oscillations in solvation forces between confining surfaces that are observed in the results of atom-force microscopy and surface-force apparatus for alkane chains.[14,24,29,43,55] It should be noted that a previous experimental study shows that a monolyer/bilayer transition may exist depending on the degree of cation exchange in organoclays, or the available area occupied by each alkylammonium.[38] However, in our simulation the gallery cations are completely replaced by DODDMA cations. Therefore, the DODDMA always possesses a multilayer structure with the alkyl chain within the layer structure mainly parallel to the clay surface.

Tilt Angle. The tilt angle of the alkyl chain with respect to the surface is frequently used to describe the arrangement of all-trans chains in idealized structured models. However, all-trans conformation is rarely found for the whole long hydrocarbon chains, which is further demonstrated in our simulation results. We note that different alignments exist not only along the alkyl chains but also between the chains within and out of layer structures. In this analysis, we describe the tilt angle with each segment along the chains. Therefore, we define here the tilt angle as the angle between a unit vector normal to the surface and a vector connecting two methylene CH_2 separated by two bonds along the chain.[22,56] The tilt angle ranges from zero to 90°. A zero tilt angle corresponds to a trans conformation, which indicates that the two-bond segment is normal to the surface,

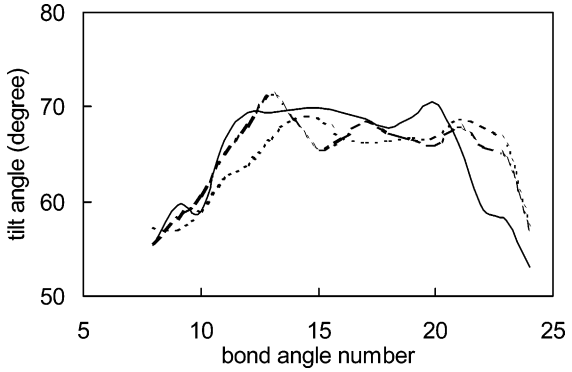

Figure 3. Tilt angle distribution of alkyl chains in DODDMA-clays as a function of bond angle number: solid curve, CEC 85 meq/100 g; dashed curve, CEC 102 meq/100 g; and dotted curve, CEC 119 meq/100 g.

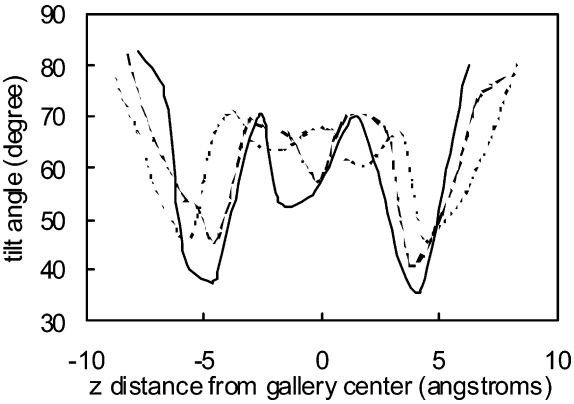

Figure 4. Tilt angle distribution of alkyl chains in DODDMA-clays as a function of *z* distance: solid curve, CEC 85 meq/100 g; dashed curve, CEC 102 meq/100 g; and dotted curve, CEC 119 meq/100 g.

and a 90° tilt angle indicates that the two-bond segment falls into the plane parallel to the surface. The tilt angles are averaged on all segments over the data collection stage and alkyl chains. The average tilt angle is around 63° in all cases, which indicates that the chains seem to be parallel to the surface. Moreover, the tilt angles close to the head and tail groups are lower than the interior ones of the chains as shown in Figure 3. The tilt angles of segments of the alkyl chains with respect to the z direction are shown in Figure 4. The tilt angle distribution is consistent with the above methylene density profiles, that is, high tilt angles are found in the position with high packing density. This further confirms that alkyl chains within the layer (corresponding to the peaks in the density profiles) have a higher tilt angle and are essentially parallel to the surface whereas the chains out of the layer structure (corresponding to the valley in the density profiles) have a smaller tilt angle.

Order Parameter. The degree of order in alkyl chains can also be analyzed quantitatively in terms of the so-called order parameter described by Leach.[57] Thus, we look into the influence of clay layer charge on the orientation of alkyl chains along the alkyl chains and normal to the clay surface. This is done via the orientation of two-bond segments that consist of three covalently-connected methylenes. The average orientational order parameter of each two-bond segment in the chains, S_{ij}, is defined by[57]

$$S_{ij} = \frac{1}{2}\langle 3\cos\theta_i \cos\theta_j - \delta_{ij}\rangle$$

where θ_i is the angle between the i^{th} local molecular axis and the surface normal (z axis), and δ_{ij} is the Kronecker delta function (equal to 1 if $i = j$ and 0 if $i \neq j$, where i and $j = x, y, z$). The angular brackets mean an average over the data collection stage (400 ps) and also over the alkyl chains within the interlayer space. The local molecular axes for the n^{th} CH_2 unit are defined as:

z: vector from C_{n-1} to C_{n+1};

y: vector, perpendicular to z, and in the plane through C_{n-1}, C_n, and C_{n+1};

x: vector, perpendicular to z and y.

The order parameter can take values ranging from 1.0 to −0.5, depending on the molecular orientation. Values close to 1.0 indicate a preference for the chosen local axis to be perpendicular to the surface whereas values close to −0.5 indicate a preference to be parallel to the surface. A value close to zero suggests a random orientation. From the diagonal elements S_{xx} and S_{yy}, the deuterium order parameter S_{CD}, which is often determined in experiments with nuclear magnetic resonance spectroscopy, can be calculated, given by

$$S_{CD} = \frac{2}{3}S_{xx} + \frac{1}{3}S_{yy}$$

For an isotropic chain which is symmetric with respect to the rotation around the local z axes, we have $S_{xx} = S_{yy}$, and $S_{xx} + S_{yy} + S_{xx} = 0$. Thus, it follows that $S_{CD} = -S_{zz}/2$. Such a chain does not have biaxial ordering since it cannot distinguish its local x and y axes.

The order parameter analysis of intercalated DODDMA clays indicates that the orientation of the interior segments in the molecular chains is different from those toward the end groups. For methylene toward the tail and head groups, the order parameter S_{zz} shown in Figure 5 tends toward zero, indicating no preferential orientation. However, for interior methylene 5−15 the negative order parameters ranging from −0.3 to −0.2 indicate that a tendency of the middle alkyl chains to align almost essentially parallel to the clay surface. With the increase of layer charge the largest differences are found for 3−4 methylenes which tend to have a tilt arrangement. A shift in order parameter is found towards the tail groups, which indicates that the segments there tend to adopt an alignment close to a horizontal arrangement. Figure 5 also compares the average S_{zz} and $-2S_{CD}$ values of the chains for the three systems with different clay layer charges. Simulation results demonstrate that the S_{zz} and $-2S_{CD}$ values are quite close, particularly in the clay system with the lowest layer charge, which indicates that there is no biaxial ordering. This equivalent relation is less valid at a higher layer charge, and the biaxiality increases as the layer charge increases. This tendency is contrary to the results obtained by Adolf et al.,[22] who found that biaxiality increases as the packing density decreases. We ascribed the biaxiality tendency in the present study to the layering behavior of alkyl chains. Note that the well-developed layer structure at the lowest layer charge in Figure 2 contributes to the no biaxial ordering.

The molecular orientation of intercalated alkyl chains within the layer structure is also found to be different from that outside of the layer structure. However, we note that the molecular orientation in the central region of the gallery is related to the clay layer charge. Figure 6 shows the order parameter of two-bond segments of the chains in the system as a function of the distance of the middle point connecting the methylenes of the segment separated by two bonds with respect to the z direction. The order parameter distribution along the z direction is consistent with the observations made for density profiles. This means that density maxima are associated with negative values

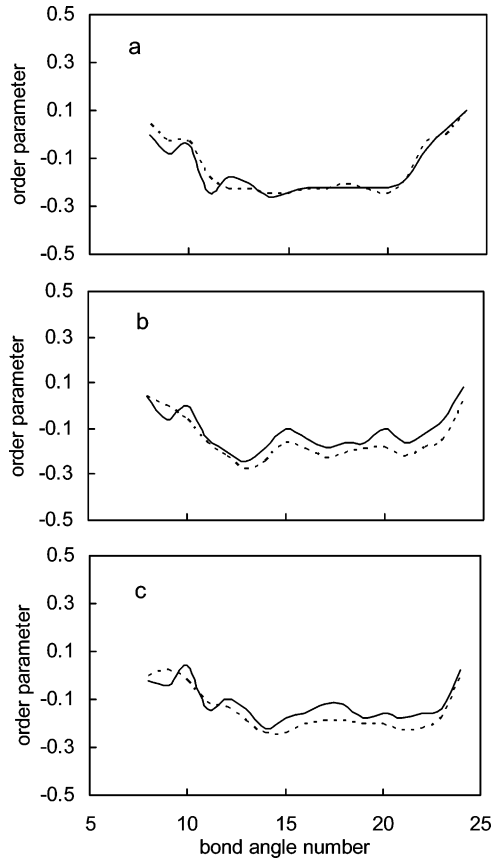

Figure 5. Order parameter distribution of alkyl chains in DODDMA-clays as a function of bond angle number. Solid curve, $-2S_{CD}$, dotted curve, S_{zz}: (a) CEC 85 meq/100 g, (b) CEC 102 meq/100 g, and (c) CEC 119 meq/100 g.

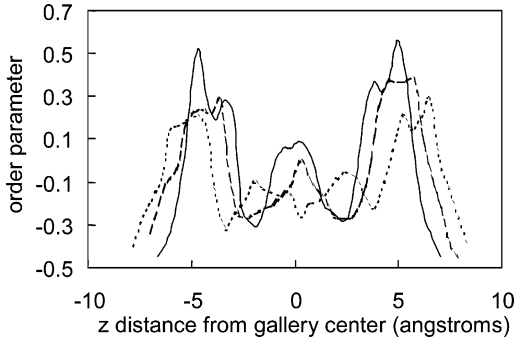

Figure 6. Order parameter (S_{zz}) distribution of alkyl chains in DODDMA-clays as a function of *z* distance: solid curve, CEC 85 meq/100 g; dashed curve, CEC 102 meq/100 g; and dotted curve, CEC 119 meq/100 g.

of order parameters. For all DODDMA−clay systems, we note the tendency of alkyl chain alignment parallel to clay surfaces within the layers and alignment perpendicular to the surfaces outside of the layers. The valleys of the order parameter distributions correspond to the layered structure displayed in density profiles whereas the peaks correspond to the structure between two layers. The large negative-order parameters in the valleys indicate that alkyl chains within each layer lie almost parallel to the surface. Meanwhile, the two peaks close to the clay surface have positive-order parameters, implying that the alkyl chains adopt a tilt arrangement between two layers. Furthermore, the order parameters in the central region are found to be related to clay layer charge. In the case of the lowest clay layer charge, the order parameters are close to zero, which indicates that the chains in the central region have no preferential orientation. In the case of a higher clay layer charge, the order parameters are around −0.1, which means the loss of orientation freedom of the chains.

Conformation. In addition to the layering behavior and orientation, a large degree of conformational freedom of the alkyl chains is expected due to the relatively small energy difference between trans and gauche conformations of alkyl chains. Actually, the coexistence of trans and gauche conformations of alkyl chains in organically-modified clays has been recently observed from FTIR and NMR spectra.[32,34,36] The NMR spectra of hexadecyltrimethylammoniums (HDTMA) show that the gauche conformation of alkyl chains becomes important upon intercalation into the clays. Figure 7 shows the initial configuration and a snapshot of DODDMA−clay after a MD simulation of 800 ps. A considerable degree of disorder in the alkyl chains within interlayer spaces can be seen in Figure 7b, which is very different from the idealized structural models in which the chains are assumed to perfectly align in completely-extended trans conformations. The methylenes in alkyl chains radiating from the same side of clay platelets are seen in Figure 7c to jump into the second and even the third layers as mentioned in the layering behavior analysis. Note that the conformation of intercalated alkyl chains depends on the charge density and structure of layered solids as well as on the temperature.[36]

We then calculated all possible conformations of the alkyl chains, restricting each torsion to the trans, gauche$^+$, and gauche$^-$ conformations. Thus, a conformation is assigned trans if it has a torsion angle of 0±60°, gauche$^+$ with an angle of −120±60°, and gauche$^-$ with an angle of 120±60°.[22,58] The average fractions of trans conformation shown in Figure 8 are in the range of 0.55−0.57. These results are comparable to the experimental studies from NMR[34] and vibrational spectra[37] on intercalated alkyl chain in layered solids and MD simulations for *n*-butane where a dominant trans conformation is observed for the methylene units.[59,60] In addition to the trans conformation, the alkyl chains also exhibit a significant amount of gauche conformation. The existence of the gauche conformation of alkyl chains intercalated into layered solids can be attributed to the looser packing of alkyl chains and the weaker steric repulsion between them as compared to the crystalline phase.

Figures 9 and 10 show the dependence of torsion angle distribution on torsion number at different temperatures. The fraction of trans conformations in all cases indicates a similar behavior. An odd−even effect is observed and is most prominent for torsion numbers close to head and tail groups. This effect indicates that the three successive bonds are arranged as a gauche−trans−gauche or trans−gauche−trans torsion angle, which enables the three-bond segments close to the head and tail to remain perpendicular to the surface. Moreover, with the increase in temperature, the fraction of gauche conformation is slightly increased indicating that the alkyl chains adopt a more disordered structure, which is in agreement with the tendency observed in the previous FTIR and NMR studies.[32,34]

Dynamics. The diffusion constant (D) is one of the most readily observable dynamic properties in a MD simulation. The diffusion constant is related to the time-dependent mean-squared displacement (MSD), $r^2(t)$, and can be calculated simply from the slope of the linear region of the MSD versus a time plot according to the Brownian motion theory:[52]

$$\langle |r_i(t) - r_i(0)|^2 \rangle = 2FDt$$

where $r_i(t)$ is the position of the i^{th} atom in the alkyl chains at time t. F is the number of dimensions in which the diffusion

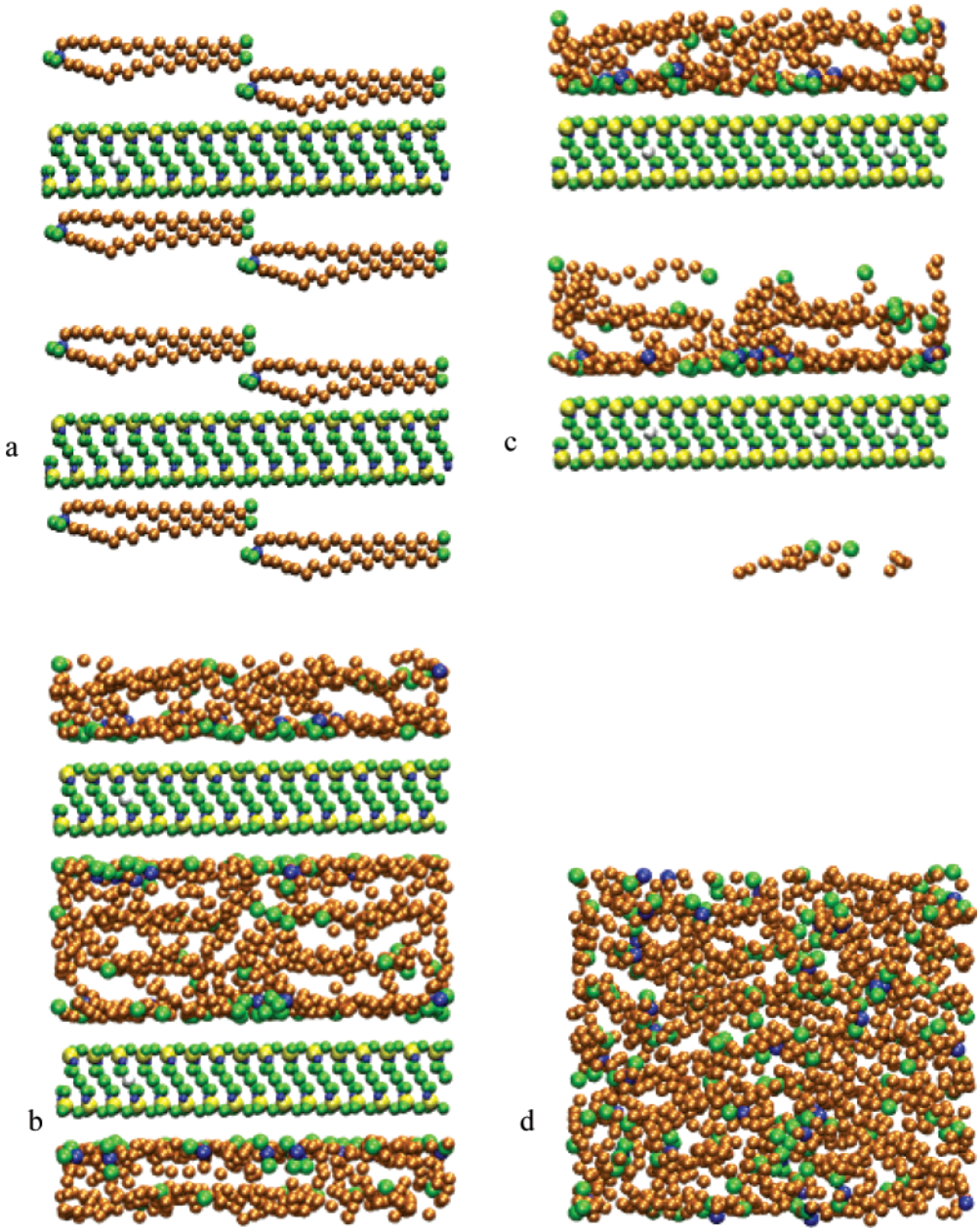

Figure 7. Simulated system consisting of 2 montmorillonite layers and 40 DODDMA chains at 300 K: (a) initial configuration; (b) snapshot at 800 ps displayed with half chains; (c) snapshot at 800 ps viewed from side; (d) top view of DODDMA chains at 800 ps. The blue balls (in DODDMA chains) are for nitrogen, the orange balls for methylene, and the green balls for methyl.

occurs; it equals 3 as three-dimensional diffusion is considered in this work. The MSDs of the selected atoms along the chains are calculated from their coordinates (x, y, z), $[x(t) - x(0)]^2 + [y(t) - y(0)]^2 + [z(t) - z(0)]^2$ in the simulation time from 400 to 700 ps (Figures 11 and 12).

The diffusion constants obtained for the intercalated alkyl chains in organoclays are in agreement with those of measured lipids, but much lower than those of simulated bulk *n*-alkane. In Figure 11 the MSDs of nitrogen and methylene are given as a function of time at different temperatures. The values calculated with the above equation are listed in Table 1. The diffusion constants are in the order of $10^{-8}-10^{-7}$ cm^2/s, which are in agreement with the values measured and derived from NMR for lipids.[61,62] However, in bulk *n*-butane a much larger diffusion constant ($6.0-6.9\times10^{-5}$ cm^2/s) is reported by Rychaert et al. Further analysis shows that the diffusion constants of both nitrogen and methylene groups increased with the system temperature. The temperature dependence of diffusion constant can be described by the Arrhenius equation:

$$D = D_0\exp(-E_{diff}/k_BT)$$

where D_0 is the pre-exponential factor which is typically weakly dependent on temperature, E_{diff} is the activation energy for diffusion and is also assumed to be a constant, k_B is equal to the Boltzmann constant and T is the temperature. As the temperature is increased, the diffusion constant increases, and the alkyl chains become more flexible and move rapidly.

The diffusion constants of atoms along the alkyl chain at 300 K are also calculated, equal to 2.3×10^{-8} cm^2/s for nitrogen; 3.3×10^{-8} cm^2/s for the first, 6.7×10^{-8} cm^2/s for the middle, and 9.3×10^{-8} cm^2/s for the end methylene; and 8.3×10^{-8} cm^2/s for the tail methyl. The nitrogen has the smallest diffusion constant, which indicates that nitrogen atoms are relatively immobile. For methylene, the diffusion constants increase along the chain from the head groups to the tail groups. The end

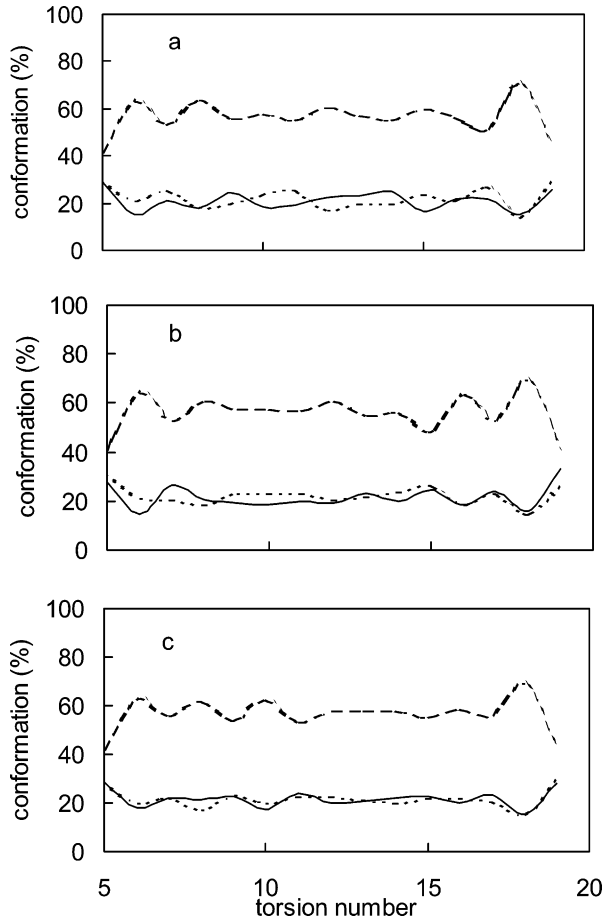

Figure 8. Conformation distribution of alkyl chains in DODDMA-clays with different CEC as a function of torsion number: (a) CEC 85 meq/100 g; (b) CEC 102 meq/100 g; and (c) CEC 119 meq/100 g. The dashed curve represents trans, the solid curve represents gauche$^+$, and the dotted curve represents gauche$^-$.

methylene has a diffusion constant about three times the value of the first methylene. Moreover, the increasing tendency of the diffusion constant along the chain suggests that methylenes toward the tail have higher mobility. The simulation results agree with the NMR study on cetyltrimethylammonium intercalated cadmium thiophosphate, which showed that the head group is immobile while the alkyl chain undergoes rapid motion.[37]

Conclusions

MD simulation provides a quantitative insight into the structure and dynamics of DODDMA chains intercalated into layered clays. A strong layering behavior with a pseudoquadrilayer structure is observed in these nanoconfined quaternary ammoniums containing two long alkyl chains. The orientation of alkyl chains in these systems varies along the chains, within and out of the layer structure. The nitrogens are mainly located within two layers close to the clay surface whereas methylenes form a pseudoquadrilayer structure, which, combined with the density oscillation normal to the clay surface, can explain the measured oscillation in solvation forces. The results of tilt angle and order parameter show that interior two-bond segments in alkyl chains prefer an arrangement parallel to the clay surface whereas the segments toward end groups adopt a random orientation. In addition, the alkyl chain segments within the layer structure lie almost parallel to the clay surface whereas those outside of the layers are essentially perpendicular to the surface. The trans conformations are predominant in all cases although

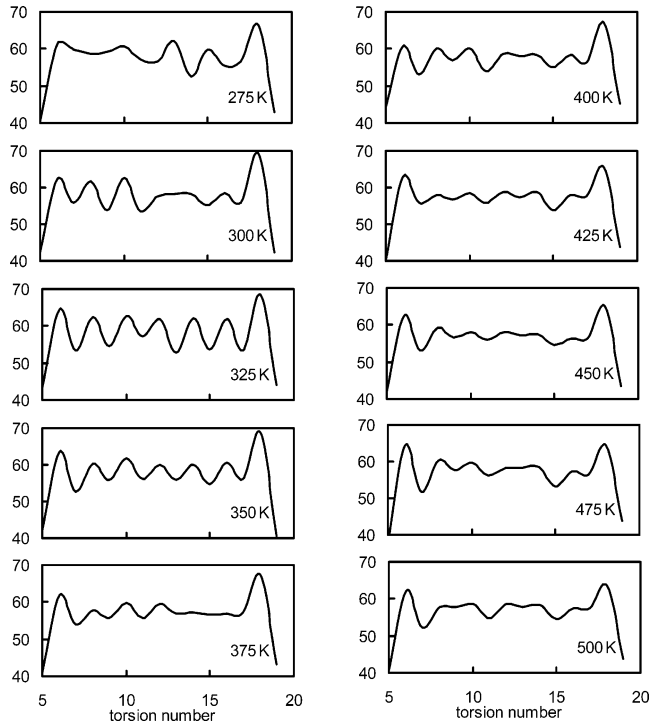

Figure 9. Trans conformation distribution of alkyl chains in DOD-DMA-clays with CEC 119 as a function of torsion number under different temperatures.

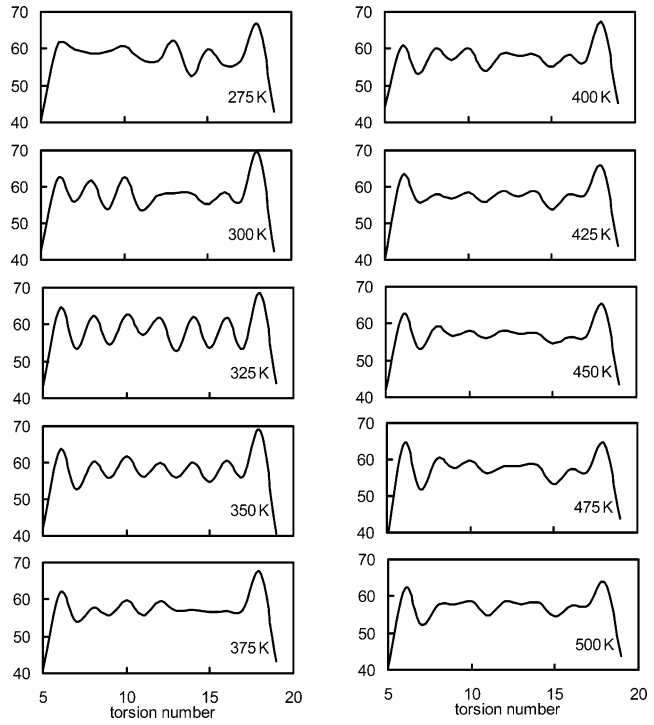

Figure 10. Gauche conformation distribution of alkyl chains in DODDMA-clays with CEC 119 as a function of torsion number under different temperatures.

extensive gauche conformations are also observed. This chain conformation is in agreement with experimental studies as well as the previous simulations on *n*-butane. Moreover, an odd−even effect in conformation is observed especially along the chains close to the head and tail groups. The nitrogen atoms are relatively immobile, whereas the mobility of methylene increases along the chain from the head groups to the tail groups. The diffusion constants of both nitrogen and methylene in the

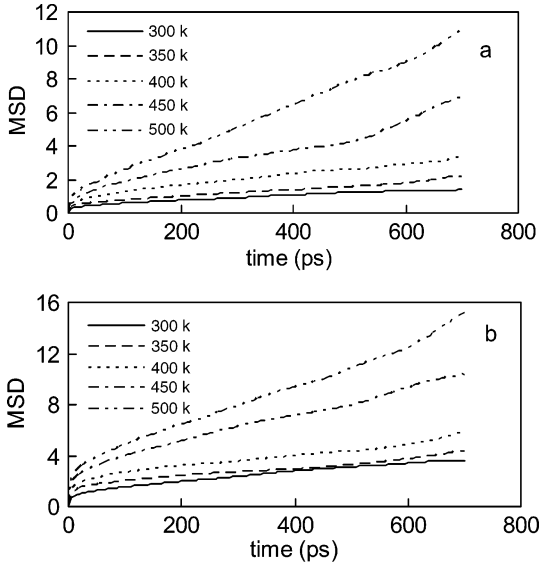

Figure 11. MSD of nitrogen and methylene as a function of time at different temperatures: (a) nitrogen and (b) methylene.

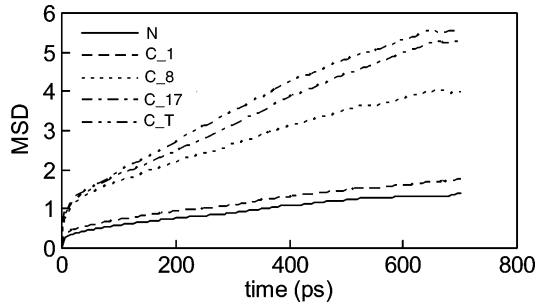

Figure 12. MSD of atoms along the chains as a function of time at 300 K.

TABLE 1: Diffusion Constants of Nitrogen and Methylene at Different Temperature

temperature, K	300	350	400	450	500
D (N), 10^{-8}cm^2/s	3.3	3.7	6.0	7.7	23.0
D (CH_2), 10^{-8}cm^2/s	5.7	5.0	7.0	13.0	20.0

chains increase with the temperature and methylene position toward the tail groups. Our results indicate that MD simulation is an effective method to investigate the nanoconfined molecular behavior of alkyl chains in organoclays. Further work has been planned to study the polymer clay nanocomposites aiming to establish the structure−property relationship for these promising novel nanostructured materials.

Acknowledgment. The authors are grateful to the Australian Research Council, University of New South Wales and University of Queensland for the financial support of the work, and the Australian Centre for Advanced Computing and Communications for the use of a SGI supercomputer. The simulation images are made with VMD, a molecular visualization program developed with NIH support by the Theoretical and Computational Biophysics group at the Beckman Institute, University of Illinois at Urbana-Champaign.

References and Notes

(1) Whittingham, M. S.; Jacobson, A. *Intercalation Chemistry*; Academic Press: New York, 1982.
(2) Ogawa, M.; Kuroda, K. *Bull. Chem. Soc. Jpn.* **1997**, *70*, 2593.
(3) Kryszewski, M. *Synth. Met.* **2000**, *109*, 47.
(4) Li, Y. Q.; Ishida, H. *Langmuir* **2003**, *19*, 2479.
(5) Zeng, Q. H.; Yu, A. B.; Lu, G. Q. (Max). In Proceedings of the ACUN−3: Technology Convergence in Composites Application; Bandyopadhyay, S., Gowripalan, N., Drayton, N., Eds.; Sydney, Australia, 2001, p 331.
(6) Zeng, Q. H.; Wang, D. Z.; Yu, A. B.; Lu, G. Q. (Max). *Nanotechnology* **2002**, *13*, 549.
(7) Bhushan, B.; Israelachvili, J. N.; Landman, U. *Nature* **1995**, *374*, 607.
(8) Kumar, S. K.; Vacatello, M.; Yoon, D. Y. *J. Chem. Phys.* **1988**, *89*, 5206.
(9) Mansfield, K. F.; Theodorou, D. N. *Macromolecules* **1989**, *22*, 3143.
(10) Bitsanis, I.; Hadziioannou, G. *J. Chem. Phys.* **1990**, *92*, 3827.
(11) Vacatello, M.; Yoon, D. Y. *J. Chem. Phys.* **1990**, *93*, 779.
(12) Kumar, S. K.; Vacatello, M.; Yoon, D. Y. *Macromolecules* **1990**, *23*, 2189.
(13) Smith, G. D.; Yoon, D. Y.; Jaffe, R. L. *Macromolecules* **1992**, *25*, 7011.
(14) Ribarsky, M. W.; Landman, U. *J. Chem. Phys.* **1992**, *97*, 1937.
(15) Xia, T. K.; Landman, U. *Science* **1993**, *261*, 5126.
(16) Klatte, S. J.; Beck, T. L. *J. Phys. Chem.* **1993**, *97*, 5727.
(17) Wang, Y.; Hill, K.; Harris, J. G. *J. Phys. Chem.* **1993**, *97*, 9013.
(18) Winkler, R. G.; Matsuda, T.; Yoon, D. Y. *J. Chem. Phys.* **1993**, *98*, 729.
(19) Padilla, P.; Toxvaerd, S. *J. Chem. Phys.* **1994**, *101*, 1490.
(20) Winkler, R. G.; Hentschke, R. *J. Chem. Phys.* **1994**, *100*, 3930.
(21) Matsuda, T.; Smith, G. D.; Winkler, R. G.; Yoon, D. Y. *Macromolecules* **1995**, *28*, 165.
(22) Adolf, D. B.; Tildesley, D. J.; Pinches, M. R. S.; Kingdon, J. B.; Madden, T.; Clark, A. *Langmuir* **1995**, *11*, 237.
(23) Dijkstra, M. *Europhys. Lett.* **1997**, *37*, 281.
(24) Gao, J. P.; Luedtke, W. D.; Landman, U. *J. Chem. Phys.* **1997**, *106*, 4309.
(25) Hackett, E.; Manias, E.; Giannelis, E. P. *J. Chem. Phys.* **1998**, *108*, 7410.
(26) Newman, S. P.; Di Cristina, T.; Coveney, P. V. *Langmuir* **2002**, *18*, 2933.
(27) Israelachvili, J. N.; Kott, S. J. *J. Chem. Phys.* **1988**, *88*, 7162.
(28) Horn, R. G.; Israelachvili, J. N. *Macromolecules* **1988**, *21*, 2836.
(29) Christenson, H. K.; Gruen, D. W. R.; Horn, R. G.; Israelachvili, J. N. *J. Chem. Phys.* **1987**, *87*, 1834.
(30) Borja, M.; Dutta, P. K. *J. Chem. Phys.* **1992**, *96*, 5434.
(31) Basini, L.; Raffaelli, A.; Zerbi, G. *Chem. Mater.* **1990**, *2*, 679.
(32) Vaia, R. A.; Teukolsky, R. K.; Giannelis, E. P. *Chem. Mater.* **1994**, *6*, 1017.
(33) Li, Y. Q.; Ishida, H. *Chem. Mater.* **2002**, *14*, 1398.
(34) Wang, L. Q.; Liu, J.; Exarhos, G. J.; Flanigan, K. Y.; Bordia, R. *J. Phys. Chem. B* **2000**, *104*, 2810.
(35) Li, Y. Q.; Ishida, H. *Langmuir* **2003**, *19*, 2479.
(36) Kubies, D.; Jerome, R.; Grandjean, J. *Langmuir* **2002**, *18*, 6159.
(37) Suresh, R.; Vasudevan, S.; Ramanathan, K. V. *Chem. Phys. Lett.* **2003**, *371*, 118.
(38) (a) Lagaly, G. *Solid State Ionics* **1986**, *22*, 43. (b) Favre, H.; Lagaly, G. *Clay Miner.* **1991**, *26*, 19.
(39) Bitsanis, I. A.; Pan, C. M. *J. Chem. Phys.* **1993**, *99*, 5520.
(40) Manias, E.; Subbotin, A.; Hadziioannou, G.; ten Brinke, G. *Mol. Phys.* **1995**, *85*, 1017.
(41) Manias, E.; Hadziioannou, G.; ten Brinke, G. *Langmuir* **1996**, *12*, 4587.
(42) Tsekov, R.; Smirniotis, P. G. *J. Phys. Chem. B* **1998**, *102*, 9385.
(43) Bhide, S. Y.; Yashonath, S. *J. Am. Chem. Soc.* **2003**, *125*, 7425.
(44) Zeng, Q. H.; Yu, A. B.; Lu, G. Q.; Standish, R. K. *Chem. Mater.* **2003**, *15*, 4732.
(45) Viani, A.; Gualtieri, A. F.; Artioli, G. *Am. Mineral.* **2002**, *87*, 966.
(46) Moraru, V. N. *Appl. Clay Sci.* **2001**, *19*, 11.
(47) Ogawa, M.; Aono, T.; Kuroda, K.; Kato, C. *Langmuir* **1993**, *9*, 1529.
(48) Mayo, S. L.; Olafson, B. D.; Goddard, W. A., III *J. Phys. Chem.* **1990**, *94*, 8897.
(49) Skipper, N. T.; Refson, K.; McConnell, J. D. C. *J. Chem. Phys.* **1991**, *94* (11), 7434.
(50) Rappe, A. K.; Goddard, W. A., III. *J. Phys. Chem.* **1991**, *95*, 3358.
(51) Forester, T. R.; Smith, W. *DL_POLY Molecular Dynamics Code*, CCP5 of the EPSRC; 1995.
(52) Allen, M. P.; Tildesley, D. J. *Computer Simulation of Liquid*; Clarendon Press: Oxford, 1989.
(53) Hoover, W. G. *Phys. Rev. A.* **1985**, *31* (3), 1695.
(54) Fornes, T. D.; Yoon, P. J.; Hunter, D. L.; Keskkula, H.; Paul, D. R. *Polymer* **2002**, *43*, 5915.
(55) Gupta, S.; Koopman, D. C.; Westermann-Clark, G. B.; Bitsanis, I. A. *J. Chem. Phys.* **1994**, *100*, 8444.
(56) Smith, P.; Lynden-Bell, R. M.; Earnshaw, J. C.; Smith, W. *Mol. Phys.* **1999**, *96*, 249.

(57) Leach, A. R. *Molecular Modeling: Principles and Applications*; Longman: London, 1996.
(58) Yoon, D. Y.; Smith, G. D.; Matsuda, T. *J. Chem. Phys.* **1993**, *98*, 10037.
(59) (a) Ryckaert, J. P.; Bellemans, A. *Chem. Phys. Lett.* **1975**, *30*, 123. (b) Ryckaert, J. P.; Bellemans, A. *Discuss. Faraday Soc.* **1978**, *66*, 95.
(60) Wielopolski, P. A.; Smith, E. R. *J. Chem. Phys.* **1986**, *84* (12), 6940.
(61) Small, D. M. *The Physical Chemistry of Lipids: from Alkanes to Phospholipids*; Plenum Press: New York, 1986.
(62) Rommel, E.; Noack, F.; Meier, P.; Kothe, G. *J. Phys. Chem.* **1988**, *92*, 2981.